ChemComm

COMMUNICATION

View Article Online
View Journal

Check for updates

Cite this: DOI: 10.1039/d5cc00170f

Received 11th January 2025,
Accepted 19th February 2025

DOI: 10.1039/d5cc00170f

rsc.li/chemcomm

Published on 19 February 2025. Downloaded by Shanghai Normal University on 2/27/2025 12:31:58 AM.

A sensitive miRNA detection method based on a split-T7 switch modulating CRISPR/Cas12a system†

Dayong Li,[a] Wenting Cheng,[a] Feifan Yin,[a] Yanheng Yao,[a] Zhongyun Wang*[c] and Yang Xiang *[ab]

This study presents a novel method for sensitive miRNA detection based on a split-T7 switch modulating CRISPR/Cas12a system. By integrating the split-T7 promoter-mediated transcription with the CRISPR/Cas12a system, this method can achieve femtomolar detection of the target miRNA within 1 h and successfully analyze miR-21 in samples from various cell lines, demonstrating its potential for clinical applications.

MicroRNA is an endogenous noncoding RNA with a length of approximately 19–24 nucleotides, which plays an important role in a series of life activities by regulating gene expression.[1,2] Different types of diseases display their unique miRNA expression characteristics.[3–5] In addition, there are also trace amounts of circulating miRNAs in biological fluids such as blood and saliva.[6,7] As the main technology for miRNA detection, polymerase chain reaction (PCR) can guarantee sensitivity and specificity, but it still relies on expensive thermal cycling devices and takes a long time, which greatly limits its application in miRNA real-time detection.[8–11]

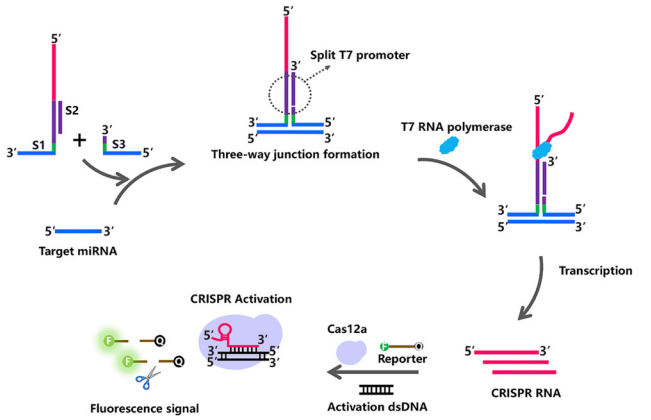
Clustered regularly interspaced short palindromic repeat and associated protein (CRISPR/Cas) has been widely used in the field of *in vitro* diagnosis because of its unique target gene recognition ability and trans-cleavage activity.[12–15] Among them, the CRISPR/Cas12a system has received much attention. The CRISPR/Cas12a can recognize and bind specific target DNA with the help of CRISPR RNA (CrRNA). Moreover, the binding of the target can activate the trans-cleaving activity of Cas12a protein, and then arbitrarily cut ssDNA in the surrounding environment.[16–18] Based on this property, researchers have combined it with isothermal amplification technology to develop a series of new methods for miRNA detection.[19–21] However, these methods often require the design of a CrRNA for detecting target genes and activating the CRISPR/Cas12a system by amplifying a specific DNA sequence and binding it with CrRNA.[22,23] Nevertheless, the high synthesis cost, susceptibility to degradation, as well as requirements for stringent storage and transportation conditions significantly restrict the application of these methods. In addition, these methods usually need to amplify the initial sequence of miRNA first, and due to the short sequence of miRNA itself, it is difficult to design primers in the process of reverse transcription and amplification, and it is easy to cause insufficient specificity.

In this work, we integrated the split-T7 promoter-mediated transcription with the CRISPR/Cas12a system to propose an innovative general-purpose strategy for detecting miRNAs.[24,25] We constructed a unique three-way junction structure. Under the influence of the approach binding effect, the appearance of the target miRNA can induce the self-assembly of the three-way junction to form a complete transcription template, and then directly transcribes the CrRNA of the downstream CRISPR/Cas12a system under the action of T7 RNA polymerase. Finally, the CRISPR fluorescence system was activated to achieve fluorescence analysis of the target miRNA. By combining transcription and the CRISPR/Cas12a system, we solve the problem of CrRNA synthesis and use in CRISPR/Cas12a detection technology, and improve the detection sensitivity by means of double signal amplification. Furthermore, the use of the three-way junction structure can effectively avoid the amplification of miRNA itself and solve the problems of primer design and lack of specificity caused by short miRNA sequences in other amplification methods. We used this method to achieve rapid detection of miR-21 within 1 h with a detection limit as low as 43.9 fM, and other miRNAs could be detected by simply replacing the sequence of the recognition region. In addition, the method can successfully analyze miR-21 in different tumor cell lines. Its rapid, sensitive and universal characteristics

[a] State Key Laboratory of Pharmaceutical Biotechnology, School of Life Sciences, Nanjing University, Nanjing 210023, P. R. China. E-mail: xiangy@nju.edu.cn
[b] State Key Laboratory of Natural and Biomimetic Drugs, Peking University, Beijing 100191, P. R. China
[c] Department of Anesthesiology, The First Affiliated Hospital of Nanjing Medical University, Nanjing 210029, P. R. China. E-mail: zywang1970@126.com

† Electronic supplementary information (ESI) available. See DOI: https://doi.org/10.1039/d5cc00170f

Published on 19 February 2025. Downloaded by Shanghai Normal University on 2/27/2025 12:31:58 AM.



Scheme 1 Schematic illustration of the proposed method for miRNA analysis.

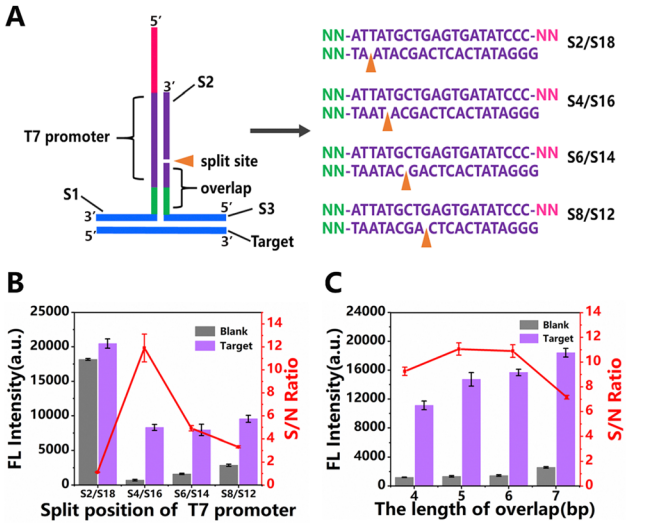


Fig. 1 Construction and optimization of the three-way junction structure. (A) Schematic diagram of the three-way junction structure and comparison of four different types of split-T7 promoter sequences (S2/S18, S4/S16, S6/S14, S8/S12). (B) Comparison of the detection results of four different three-way junction structures. (C) Optimization of the length of complementary overlapping regions of S1 and S3. The concentration of S1, S2 and S3 for each type of split-T7 promoter sequences is 10 nM. The concentration of the target is 100 pM. The transcription is performed at 37 °C for 20 min, then at 70 °C for 5 min. The CRISPR reaction time is 10 min. Error bars: standard deviation (SD), n = 3.

fully indicate that the method has great clinical application potential.

As shown in Scheme 1, the actual detection process of the method is mainly divided into two steps: target-induced transcription process and CRISPR fluorescence analysis. We designed three DNA probes as target recognition elements including S1, S2 and S3. Among them, S1 mainly includes three functional regions: transcriptional template sequence (pink region), T7 promoter sequence (purple region) and partial recognition sequence of target miRNA (blue region). S2 contains a partial sequence of the T7 promoter (purple region), which complements S1 to form a double strand. The sequences on S3 are mainly the partial T7 promoter sequence (purple region) and partial target miRNA recognition sequence (blue region). When there is no target, the T_m value of the complementary region of S3 and S1 is too small, and S1 cannot be complementary to S3 at the reaction temperature of 37 °C, so S1, S2 and S3 cannot be combined to form a complete T7 promoter, and the transcription reaction cannot proceed at this time. When the target miRNA appears, the target binds to the target recognition region of S1 and S3, respectively, which leads to the proximity of S1 and S3. At this time, S1 and S3 can stably bind together with S2 to form a three-way junction with complete T7 promoter sequence. Subsequently, T7 RNA polymerase binds to the promoter and transcribes a large number of RNA products. The transcription sequence (pink region) on S1 is pre-designed as a complementary sequence to the CrRNA of the downstream CRISPR/Cas12a system, so that the final transcribed RNA product can be directly used as the CrRNA. After transcription, CrRNA binds to Cas12a protein and initiates the *trans*-cleavage activity of Cas12a protein under the action of activation DNA. By cutting the fluorescent reporter, a significant fluorescence signal is generated, so as to realize the detection of target miRNA.

The complete T7 promoter is a 20-nucleotide dsDNA sequence that can be specifically recognized by T7 RNA polymerase to initiate transcription. In our design, the presence of the target miRNA can induce the three-way junction self-assembly of the DNA recognition probe to form a stable T7 promoter with a nick. Then the input signal of upstream miRNA is converted into the output signal of downstream RNA through the transcription reaction mediated by the split-T7 promoter, which is the most critical step in the whole detection process. Therefore, we first investigated the influence of the split location of the T7 promoter on the analysis effect. We designed four groups of recognition probes for a synthetic DNA target and assembled them into T7 promoter transcription templates containing different split sites, including S2/S18, S4/S16, S6/S14 and S8/S12 (Fig. 1A). Then the CRISPR fluorescence analysis system was combined to analyze the final detection effect. As shown in Fig. 1B, when the split site is two nucleotides away from the 5′ end of the promoter (S2/S18 type), strong fluorescence signals are generated regardless of the presence or absence of the target, and the signal-to-noise (S/N) ratio is extremely low. However, when the split position moved two nucleotides to the 3′ end (S4/S16 type), the background signal decreased significantly, and the S/N ratio was the highest. In addition, when the split site continues to move to the 3′ end (S6/S14 and S8/S12 types), the background signal gradually increases, and the S/N ratio decreases sharply. Based on these results, we selected type S4/S16 split promoter probes for subsequent studies.

The successful self-assembly of the three-way junction structure determines the effective formation of the transcriptional promoter. In the design of this method, the complementary overlapping regions of S3 and S1 probes are too short and the T_m value is low, so they can approach to form a complete three-way junction structure only in the presence of the target. Here, we optimize the length of the complementary regions of S3 and S1. As shown in Fig. 1A and C, we compared the detection effect by adding additional nucleotide sequences to

 This journal is © The Royal Society of Chemistry 2025

Published on 19 February 2025. Downloaded by Shanghai Normal University on 2/27/2025 12:31:58 AM.

the S4/S16 type probes. The results showed that when the complementary length was 5–6 nucleotides, the detection effect was the best and the S/N ratio was the highest. However, when the complementary length reached 7 nucleotides, the background signal increased significantly and the S/N ratio decreased. Therefore, we set the complementary length of S3 and S1 probes as 5 nucleotides.

After a series of investigations, we took miR-21 as the model target to verify the feasibility of this method for miRNA detection. We first used polyacrylamide gel electrophoresis to test whether miR-21 can trigger three-way junction self-assembly of DNA recognition probes. As shown in Fig. S1A (ESI†), the target miR-21 can not only stably bind to S1 and S2 complexes, but also hybridize with the target recognition sequence of S3. In addition, in the absence of target miR-21, S1, S2, and S3 could not self-assemble to form a three-way junction transcription template. However, when the target miR-21 and the DNA probe were present at the same time, stable bands with higher molecular weights appeared in lane 6, which proved that the target could successfully trigger the three-way junction self-assembly of the DNA recognition probe. Next, we performed gel electrophoresis analysis on the transcripts of the three-way junction transcription template, as shown in Fig. S1B (ESI†). Compared with the transcription template in lane 1, many new bands were generated in lane 2. In addition, compared with the synthetic CrRNA in lane 3, bands also appeared at the position of CrRNA in lane 2, indicating that the split-T7 promoter can effectively initiate the transcription and transcribe the corresponding CrRNA products. Finally, we introduced the CRISPR/Cas12a fluorescence system to verify the feasibility of this method for the detection of miR-21. The results of fluorescence spectroscopy in Fig. S1C (ESI†) showed that only when the target miRNA was present could significant fluorescence signals be generated, while no obvious signals were generated in other parallel controls. In conclusion, the above experimental results fully prove the feasibility of this method for miRNA detection.

In order to improve the detection performance of this method, we optimize some experimental conditions. We first optimized the concentration of DNA probes. As shown in Fig. S2A (ESI†), when the concentration of DNA probes was 5 nM, the S/N ratio was the largest, so we set the concentration of DNA probes to 5 nM. Subsequently, we optimized the concentration of T7 RNA polymerase, and the experimental results showed that 20 U of RNA polymerase could achieve the best detection effect (Fig. S2B, ESI†). In addition, we found that the signal intensity reached the highest level when the concentration of magnesium ions (Mg^{2+}) exceeded 10 mM (Fig. S3A, ESI†). Next, we explored the temperature of the transcription reaction, as shown in Fig. S3B (ESI†). The best effect was achieved when the reaction temperature was 37 °C. Finally, we optimized the time of transcription. As shown in Fig. S3C (ESI†), the fluorescence signal peaked at about 30 min and then tended to stabilize.

Next, we tested the sensitivity of the method to detect miR-21 under optimal conditions. We used this method to analyze the fluorescence spectra and signal intensities in samples containing different concentrations of the target. As shown in Fig. 2A and B, the fluorescence signal intensity gradually increased with the increase of target concentration, showing a positive correlation between the two. Moreover, there is a good linear relationship between fluorescence intensity and the logarithm of target concentration in the range of 100 fM–1 nM (Fig. 2C). After derivation, the corresponding equation is calculated as $y = 4849.29x - 5905.82$, and the detection limit is 43.9 fM. Compared with some previously proposed miRNA detection methods, the analytical performance of this method has obvious advantages (Table S2, ESI†).

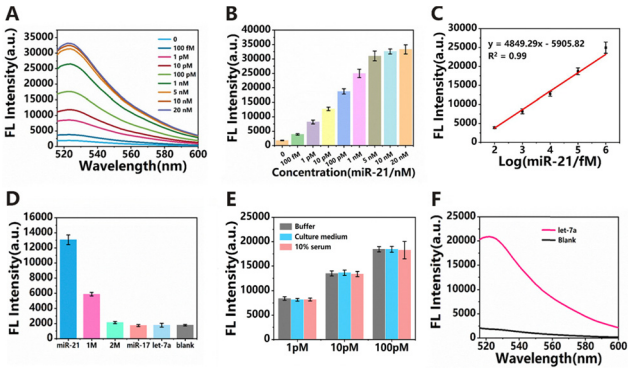


Fig. 2 (A) Fluorescence spectra corresponding to different concentrations of miR-21 (excitation wavelength: 485 nm; emission wavelength: 525 nm). (B) Fluorescence intensity generated by different concentrations of miR-21 (0, 100 fM, 1 pM, 10 pM, 100 pM, 1 nM, 5 nM, 10 nM, and 20 nM). (C) Linear relationship between fluorescence intensity and the logarithm of miR-21 concentration (100 fM, 1 pM, 10 pM, 100 pM, and 1 nM). The *y*-axis refers to the fluorescence intensity, the *x*-axis refers to the logarithm of miR-21 concentration. (D) Selectivity study of the method. The concentration of miR-21, single-base mutant miR-21 (1M) and double-base mutant miR-21 (2M) is 100 pM, and the concentration of miR-17 and let-7a is 1 nM. (E) Stability test of the method (normal reaction buffer, 10% serum and 10% culture medium). (F) Validation of the generality of the method. Fluorescence spectra corresponding to the 100 pM let-7a target and blank group. The transcription time is 30 min. The CRISPR reaction time is 20 min. Error bars: standard deviation (SD), $n = 3$.

The sequence homology of miRNA poses a challenge to the specificity of detection methods. We tested the specificity of the method by setting up control groups of single-base mutant miR-21 (1 M), double-base mutant miR-21 (2 M), let-7a and miR-17. As shown in Fig. 2D, compared with miR-21, the fluorescence intensity of 1 M decreased by more than 60%, while there was no significant difference between 2 M and the blank control. In addition, two non-homologous miRNA controls (let-7a, miR-17) also did not show significant signals. These results show that the method has good selectivity.

Next, we tested the detection stability of this method. We selected 10% serum and 10% culture medium as complex substrates for comparison with ordinary buffers. As shown in Fig. 2E, the changes of fluorescence signals in the three different analysis environments were basically the same, with no significant difference. In addition, we conducted recovery experiments on different substrates and obtained recoveries ranging from 93.8% to 106% (Table S3, ESI†). These results show that the method can maintain good stability in complex biological substrates. Finally, we verify the generality of the

Published on 19 February 2025. Downloaded by Shanghai Normal University on 2/27/2025 12:31:58 AM.

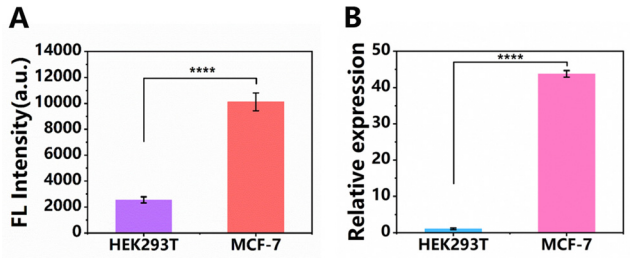


Fig. 3 (A) Fluorescence intensity of miR-21 in breast cancer cells (MCF-7) and human embryonic kidney cells (HEK293T). Statistical significance is calculated by the *t*-test (****, $p < 0.0001$). (B) The relative expression of miR-21 in breast cancer cells (MCF-7) and human embryonic kidney cells (HEK293T) by standard RT-qPCR. Statistical significance is calculated by the *t*-test (****, $p < 0.0001$). The relative expression of miR-21 was calculated by $2^{-\Delta\Delta Ct}$. The U6 RNA was used as the internal reference gene for miRNA-21. Error bars: standard deviation (SD), $n = 3$.

method. We selected let-7a as the target for verification. As shown in Fig. 2F, the effective analysis of let-7a can be achieved by simple substitution of the recognition sequence, indicating that this method can be used for the general detection of miRNA.

Previous studies have shown that miR-21 is highly expressed in breast cancer cells. To further illustrate the practical application potential of this method, we cultured the breast cancer cell line (MCF-7) and human embryonic kidney cell line (HEK293T), and used this method to detect miR-21 in the two different cell lines. As shown in Fig. 3A, the fluorescence signal obtained from breast cancer cell samples was significantly stronger than that of human embryonic kidney cell samples, indicating that the expression of miR-21 in MCF-7 was higher than that in HEK293T. In addition, as shown in Fig. 3B and Fig. S4 (ESI†), we compared the detection results of this method with gold standard RT-qPCR, and the results were highly consistent, proving that this method has great clinical application potential.

In this study, we have integrated the split-T7 promoter-mediated transcription with the CRISPR/Cas12a system to establish a rapid and sensitive method for miRNA analysis. The innovative design of the split-T7 promoter structure in this method directly converts the target recognition signal into self-assembly of the transcription template, eliminating the need for primer design and reverse transcription in miRNA detection. By coupling the split-T7 promoter with the CRISPR/Cas12a system, the method can initiate the downstream CRISPR/Cas12a system through a specific CrRNA product. This not only addresses cost concerns associated with traditional CRISPR detection methods that use CrRNA but also achieves double cascade amplification. Our method enables sensitive detection of miR-21 within 1 h, with a detection limit as low as 43.9 fM, offering distinct advantages over other miRNA detection methods. Furthermore, our method exhibits excellent selectivity and stability, capable of identifying single-base mutations and maintaining stability in complex biological substrates. Leveraging the extensibility of the three-way junction structure allows for universal detection of different miRNA by simply modifying the recognition sequence. We have successfully applied this method to analyze miR-21 in samples from various cell lines, demonstrating its potential for clinical applications.

This work was supported by the National Natural Science Foundation of China (grant no. 82371283 and 81672570) and the State Key Laboratory of Natural and Biomimetic Drugs (grant no. K202009).

Data availability

The data supporting this article have been included as part of the ESI.†

Conflicts of interest

There are no conflicts to declare.

Notes and references

1 J. M. Moreno-Moya, F. Vilella and C. Simón, *Fertil. Steril.*, 2014, **101**, 1516–1523.
2 R. A. Naqvi, M. Datta, S. H. Khan and A. R. Naqvi, *Semin. Cell Dev. Biol.*, 2022, **124**, 34–47.
3 L. Rios-Colon, G. Deep and D. Kumar, *Tumour Biol.*, 2019, **41**, 1010428319881344.
4 M. V. Iorio and C. M. Croce, *EMBO Mol. Med.*, 2012, **4**, 143–159.
5 S. Chen, Y. Deng and D. Pan, *Viruses*, 2022, **14**, 1215.
6 E. C. Fung, A. N. Butt, J. Eastwood, R. Swaminathan and R. Sodi, *Adv. Clin. Chem.*, 2019, **91**, 99–122.
7 H. Yu, Z. Guan, K. Cuk, H. Brenner and Y. Zhang, *Cancer Med.*, 2018, **7**, 4849–4862.
8 G. A. de Ferronato, M. B. Cerezetti, A. Bridi, C. M. Prado, G. Dos Santos, N. M. Bastos, P. M. S. da Rosa, J. G. Ferst and J. C. da Silveira, *Methods Mol. Biol.*, 2023, **2595**, 159–170.
9 F. Takei, M. Akiyama, A. Murata, A. Sugai, K. Nakatani and I. Yamashita, *ChemBioChem*, 2020, **21**, 477–480.
10 M. Kotlarek, A. Kubiak, K. Jażdżewski and A. Wójcicka, *Methods Mol. Biol.*, 2018, **1823**, 69–85.
11 Y. Abel and M. Rederstorff, *Methods Mol. Biol.*, 2021, **2300**, 59–64.
12 A. Pickar-Oliver and C. A. Gersbach, *Nat. Rev. Mol. Cell Biol.*, 2019, **20**, 490–507.
13 Q. A. Phan, L. B. Truong, D. Medina-Cruz, C. Dincer and E. Mostafavi, *Biosens. Bioelectron.*, 2022, **197**, 113732.
14 J. E. van Dongen, J. T. W. Berendsen, R. D. M. Steenbergen, R. M. F. Wolthuis, J. C. T. Eijkel and L. I. Segerink, *Biosens. Bioelectron.*, 2020, **166**, 112445.
15 T. Tanny, M. Sallam, N. Soda, N. T. Nguyen, M. Alam, M. J. A. Shiddiky and J. Agric, *Food Chem.*, 2023, **71**, 11765–11788.
16 Y. Shi, X. Fu, Y. Yin, F. Peng, X. Yin, G. Ke and X. Zhang, *Chem. – Asian J.*, 2021, **16**, 857–867.
17 F. Safari, K. Zare, M. Negahdaripour, M. Barekati-Mowahed and Y. Ghasemi, *Cell Biosci.*, 2019, **9**, 36.
18 J. S. Chen, E. Ma, L. B. Harrington, M. Da Costa, X. Tian, J. M. Palefsky and J. A. Doudna, *Science*, 2018, **360**, 436–439.
19 Q. Zhang, X. Zhang, X. Zou, F. Ma and C. Y. Zhang, *Chemistry*, 2023, **29**, e202203412.
20 B. Luo, J. Zhou, X. Zhan, B. Ying, F. Lan and Y. Wu, *Talanta*, 2024, **277**, 126310.
21 R. Gao, R. Ji and W. Dong, *Talanta*, 2023, **265**, 124812.
22 W. Jiang, Z. Chen, J. Lu, X. Ren and Y. Ma, *Talanta*, 2023, **251**, 123784.
23 X. Zhang, H. Li, W. Zhao, J. Xu, S. Wang and R. Yu, *Mikrochim. Acta*, 2023, **190**, 458.
24 T. Yoon, J. Shin, H. J. Choi and K. S. Park, *Biosens. Bioelectron.*, 2022, **208**, 114221.
25 J. Shin, T. Yoon, D. Nam, D. Kim, S. Kim, B. S. Cha, E. S. Lee, Y. Jang, S. Kim, J. Han, H. J. Choi and K. S. Park, *Chem. Eng. J.*, 2023, **464**, 142614.

 This journal is © The Royal Society of Chemistry 2025